

IR plus vacuum ultraviolet spectroscopy of neutral and ionic organic acid molecules and clusters: Acetic acid

Y. J. Hu, H. B. Fu, and E. R. Bernstein

Citation: *The Journal of Chemical Physics* **125**, 184308 (2006); doi: 10.1063/1.2378626

View online: <http://dx.doi.org/10.1063/1.2378626>

View Table of Contents: <http://aip.scitation.org/toc/jcp/125/18>

Published by the *American Institute of Physics*

COMPLETELY

REDESIGNED!



**PHYSICS
TODAY**

Physics Today Buyer's Guide
Search with a purpose.

IR plus vacuum ultraviolet spectroscopy of neutral and ionic organic acid molecules and clusters: Acetic acid

Y. J. Hu, H. B. Fu, and E. R. Bernstein^{a)}

Department of Chemistry, Colorado State University, Fort Collins, Colorado 80523-1872

(Received 14 August 2006; accepted 5 October 2006; published online 10 November 2006)

Infrared (IR) vibrational spectroscopy of acetic acid (A) neutral and ionic monomers and clusters, employing vacuum ultraviolet (VUV), 10.5 eV single photon ionization of supersonically expanded and cooled acetic acid samples, is presented and discussed. Molecular and cluster species are identified by time of flight mass spectroscopy: the major mass features observed are A_nH^+ ($n = 1-9$), $ACOOH^+$ (VUV ionization) without IR radiation present, and A^+ with both IR and VUV radiation present. The intense feature $ACOOH^+$ arises from the cleavage of $(A)_2$ at the β -CC bond to generate $ACOOH^+ + CH_3$ following ionization. The vibrational spectrum of monomeric acetic acid ($2500-7500\text{ cm}^{-1}$) is measured by nonresonant ionization detected infrared (NRID-IR) spectroscopy. The fundamentals and overtones of the CH and OH stretches and some combination bands are identified in the spectrum. Mass selected IR spectra of neutral and cationic acetic acid clusters are measured in the $2500-3800\text{ cm}^{-1}$ range employing nonresonant ionization dip-IR and IR photodissociation (IRPD) spectroscopies, respectively. Characteristic bands observed at approximately $2500-2900\text{ cm}^{-1}$ for the cyclic ring dimer are identified and tentatively assigned. For large neutral acetic acid clusters $A_n(n > 2)$, spectra display only hydrogen bonded OH stretch features, while the CH modes ($2500-2900\text{ cm}^{-1}$) do not change with cluster size n . The IRPD spectra of protonated (cationic) acetic acid clusters A_nH^+ ($n = 1-7$) exhibit a blueshift of the free OH stretch with increasing n . These bands finally disappear for $n \geq 6$, and one broad and weak band due to hydrogen bonded OH stretch vibrations at approximately 3350 cm^{-1} is detected. These results indicate that at least one OH group is not involved in the hydrogen bonding network for the smaller ($n \leq 5$) A_nH^+ species. The disappearance of the free OH stretch feature at $n \geq 6$ suggests that closed cyclic structures form for A_nH^+ for the larger clusters ($n \geq 6$). © 2006 American Institute of Physics. [DOI: 10.1063/1.2378626]

I. INTRODUCTION

Intermolecular interactions between carboxylic acids are a concern for a number of chemical and biological systems.¹⁻¹¹ In crystals and liquids, carboxylic acid molecules are interlinked to form either cyclic dimers or infinite chains: the nature of this intermolecular bonding depends on the substituent R .^{1,12} Protonated carboxylic acid clusters have been generated through electron impact ionization¹³⁻¹⁵ and extensively studied with regard to unimolecular dissociation. The $(RCOOH)_nH^+$ clusters with $n \leq 5$ fragment through the release of a neutral monomer. Optimized structure calculations for these clusters corroborate this dissociation pathway.^{13,16} Open-chain structures with one or two free OH group(s) at the periphery are favored energetically for $n = 5$. Chain structures terminated by closed cyclic dimer units are preferable for $n \geq 6$.¹³⁻¹⁶

Acetic acid molecules are known to form dimers in the gas phase and this process has been extensively studied for more than 50 years. Due to the stability of the planar cyclic dimer with its two hydrogen bonds, it has been assumed to be the only important associated species in the vapor phase

of acetic acid. Vibrational spectra of the dimer have been observed approximately $2550-2800\text{ cm}^{-1}$ that present some characteristic bands assigned as combination bands of low energy modes of the cyclic dimer ring with the COH bending overtone.^{17,18} Additionally, *ab initio* calculations and experiments have been performed on the acetic acid dimer to elucidate and understand these observed spectra.^{19,20}

In the absence of resolvable electronic transitions in the visible and ultraviolet spectral ranges, vibrational spectroscopy has been the major approach to elucidation of the structure and dynamics of neutral and ionic carboxylic acid molecules and clusters.²¹⁻²⁵ This approach has also been taken to the study of alkyl alcohols,^{26,27} as well. In the present report, we present observation of vibrational spectra of acetic acid molecules and clusters generated and cooled in a supersonic expansion. Vibrational spectra are acquired over the range of $2500-7500\text{ cm}^{-1}$ employing IR plus vacuum ultraviolet (VUV) nonresonant ionization detected (NRID-IR) spectroscopy. Additionally, IR plus VUV nonresonant ion dip (NRIDip-IR) and infrared photodissociation (IRPD) spectroscopies are applied to the study of neutral and protonated acetic acid clusters, respectively. Analysis of this vibrational and time of flight mass spectroscopy (TOFMS) data leads to structural information on acetic acid clusters.

^{a)}Electronic mail: erb@lamar.colostate.edu

II. EXPERIMENTAL PROCEDURES

A. Generation and detection of acetic acid clusters

The experimental apparatus employed to record VUV/TOFMS and IR spectra has been previously described in detail,^{26–29} and thus only a brief description is given here. Acetic acid vapor is seeded into a Ne/He mixture (70:30, “first run Ne”) at a total pressure of 3 atm. The gas mixture is expanded into a vacuum chamber from a General Valve pulse nozzle under supersonic flow conditions. This molecular beam in the vacuum contains both acetic acid cold monomers and clusters. The beam is collimated by a conical skimmer with a 1.5 mm entrance aperture at its apex, located about 3 cm from the nozzle orifice. This beam is crossed perpendicularly by a 118 nm VUV laser beam at the ion source region of a TOFMS. The counter propagating (to the VUV beam) IR laser beam is focused upstream from the molecular beam/118 nm beam intersection point by a 40 cm focal length lens.

Generation of the VUV 118 nm laser light and the IR light is reported in previous publications from our laboratory.^{28,29} The VUV radiation is generated as the ninth harmonic of the fundamental of the 1.064 μm output of a Nd³⁺: YAG (yttrium aluminum garnet) laser. The fundamental 1.064 μm is tripled to 355 nm, which is focused into a cell of Xe:Ar 1:10 at approximately 250 Torr by a 25 cm lens. The 118 nm light generated is focused by a MgF₂ lens into the ionization region of a TOFMS. This same lens defocuses the residual 355 nm light. The 118 nm light is $\sim 5 \mu\text{J}/\text{pulse}$ or $\sim 10^{12}$ photons/pulse and the conversion efficiency is roughly 10^{-5} . This light is employed for single photon ionization of the molecules and clusters in the molecular beam. IR light output over the covered range is 3–5 mJ/pulse with a bandwidth of 2–3 cm^{-1} (broad band mode).

B. IR+VUV spectroscopy detection of acetic acid monomers, clusters, and their ions

The VUV (10.5 eV) single photon is not energetic enough to ionize a supersonic expansion cooled acetic acid monomer as the acetic acid ionization energy (IE) is 10.8 eV.³⁰ If the IR laser is scanned to excite the acetic acid molecule to vibrational excited states of the ground electronic state, the total energy in the molecule of ($h\nu_{\text{IR}} + h\nu_{\text{VUV}}$) is higher than the IE of acetic acid and the IR excited molecule can absorb a 10.5 eV photon and ionize. By this technique (NRID-IR), the OH and CH stretch fundamental and overtone modes are recorded as an increase in the monomer ion mass channel A^+ .

IR spectroscopy of neutral clusters and their ions is developed based on vibrational predissociation spectroscopy of weakly bound clusters.^{31–34} Previous studies on methanol clusters²⁷ demonstrate that they can be ionized by VUV (118 nm, 10.5 eV) light and that the generated $(\text{CH}_3\text{OH})_{n-1}\text{H}^+$ protonated clusters originate from their neutral parent clusters $(\text{CH}_3\text{OH})_n$. This proton transfer reaction is driven by the excess ionization energy [vertical ionization energy (VIE) versus adiabatic ionization energy (AIE)] and by the ΔH of the proton transfer reaction whose barrier must

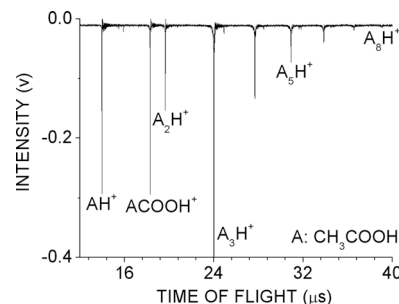


FIG. 1. TOF mass spectrum of acetic acid clusters ionized by a single photon of VUV (118 nm) light. The peaks at 24.9, 28.4, and 31.7 μs can be assigned as $(\text{CH}_3\text{COOH})_n$ ($n=3, 4,$ and 5), respectively. The feature at $\sim 31.9 \mu\text{s}$ is a background (oil?) peak.

be smaller than the (VIE)-(AIE) energy. The IE of acetic acid (10.8 eV) (Ref. 30) is close to that of methanol and similar detection can be obtained for the present system.

With the tunable IR light introduced in the experiment approximately 50 ns prior to the VUV pulse, IR absorption (multiphoton, most likely) by a cluster will induce photodissociation of the neutral $(\text{CH}_3\text{COOH})_n$ (A_n) leading to a reduction of the protonated acetic acid cluster ion $[(\text{CH}_3\text{COOH})_{n-1}\text{H}^+]$ signal related to the neutral parent cluster $(\text{CH}_3\text{COOH})_n$. Thus by scanning the IR wavelength while monitoring the $(\text{CH}_3\text{COOH})_{n-1}\text{H}^+$ mass channel signal intensity, a mass selective IR spectrum of the neutral cluster A_n is obtained as an IR in dip spectrum. This technique is called NRIDip-IR spectroscopy.

Similarly, if the tunable IR light pulse is introduced with a delay time of approximately 30 ns after the VUV laser pulse, a mass selected IR spectrum of cluster cation $A_{n-1}\text{H}^+$ is obtained as an ion dip spectrum, as the IR wavelength is scanned. This detection method is called IRPD spectroscopy. Thus to be explicit, these experiments can show two sources of cluster fragmentation. The first is due to a proton transfer reaction in the newly created A_n ion, A_n^+ . This generates the detected $A_{n-1}\text{H}^+$ cluster ion and is present without IR radiation for spectroscopy. The second source of fragmentation allows the observation of IR spectra of A_n or $A_{n-1}\text{H}^+$ on the $A_{n-1}\text{H}^+$ mass channel. This source is due to IR dissociation of the neutral cluster or protonated cluster ion probably associated with multiphoton IR absorption as the IR laser is tuned through the range of 2500–7000 cm^{-1} .^{26,27,28(d),29}

III. RESULTS AND DISCUSSION

A. VUV (118 nm) single photon ionization of acetic acid clusters

Figure 1 shows the TOF mass spectrum of acetic acid clusters employing 118 nm laser light for single photon ionization. The main cluster ion series observed is $(\text{CH}_3\text{COOH})_n\text{H}^+$ ($A_n\text{H}^+$) ($n=1-8$). The 118 nm photon energy (10.49 eV) is roughly 0.1–0.3 eV below the VIE for acetic acid. Clusters A_n have a lower IE than the acetic acid monomer, and can in general be ionized by a 118 nm photon; protonated clusters $A_{n-1}\text{H}^+$ are generated from A_n^+ cluster ions by subsequent proton transfer and fragmentation of CH_3COO . Similar results are reported for alcohol, water, and

TABLE I. Heat of the reactions obtained from calculations with B3LYP/ aug-cc-pVDZ. Calculations are carried out with default options for GAUSSIAN 03 (energy and density minimization to 10^{-4} or energy to 10^{-5} whichever comes first for the SCF program). The integrations are accomplished with a “fine” grid as default. All energies are corrected for harmonic zero point energies.

Reaction	ΔH (eV)
$(\text{CH}_3\text{COOH})_2 \rightarrow (\text{CH}_3\text{COOH})_2^+$	9.53
$(\text{CH}_3\text{COOH})_2 \rightarrow \text{CH}_3\text{COOH} + \text{COOH}^+ + \text{CH}_3$	9.72
$(\text{CH}_3\text{COOH})_2 \rightarrow \text{CH}_3\text{COOH}_2^+ + \text{CH}_3\text{COOH}$	10.56

ammonia clusters. The ΔH of the proton transfer reaction following the ionization process drives the fragmentation.^{26,27,28(d),29}

The mass spectrum of Fig. 1 evidences an additional feature identified as $\text{CH}_3\text{COOHCOOH}^+$ (ACOOH^+): this feature arises from a β -CC bond fission reaction for the dimer A_2 . A similar reaction has been characterized for ethanol and propanol in detail by Tsai *et al.*³⁵ The mass feature ACOOH^+ has almost the same intensity as the AH^+ feature also from A_2 and also generated from the ionized dimer A_2^+ [$(\text{CH}_3\text{COOH})\text{H}^+ + \text{CH}_3\text{COO}$ and $(\text{CH}_3\text{COOH})\text{COOH}^+ + \text{CH}_3$]. These two reaction channels for A_2^+ are predicted by *ab initio* calculations,³⁵ as well. Table I summarizes the heats of reaction for different dissociation channels of the acetic acid dimer, as generated by calculations, but does not give reaction path surfaces or channel barriers. Thus, two pathways are identified for the ion molecule reaction for the dimer under VUV, single photon ionization. Note that the $\text{CH}_3/\text{ACOOH}^+$ reaction channel is not open for larger clusters ($n > 2$). This observation implies that the proton affinities (PA) of larger clusters are larger than those of A_n ($n = 1, 2$), and these larger PAs favor the proton transfer channel over the β -CC cleavage channel for the cluster ion A_n^+ .

B. IR+VUV (118 nm) nonresonant ionization detected (NRID-IR) spectroscopy of the acetic acid monomer

As pointed out above, a 118 nm (10.5 eV) single photon cannot ionize a cold acetic acid monomer. With addition of vibrational excitation of the monomer in the mid-IR range (0.35–0.7 eV), the total energy in the molecule will exceed its VIE and hence the molecule can ionize. The mass spectrum of Fig. 2(a) shows that this is indeed the case. Given this fact, IR+VUV NRID-IR spectroscopy has been applied to obtain the vibrational spectrum of acetic acid in the mid-IR range (2500–7500 cm^{-1}). This spectrum is shown in Fig. 2(b): features located at approximately 3585 and 6999 cm^{-1} are due to the OH fundamental stretch (ν_{OH}) and its first overtone ($2\nu_{\text{OH}}$), respectively,^{36,37} the four features located near 3000 cm^{-1} can be identified as CH fundamental stretches (ν_{CH}), and the features approximately 6000 cm^{-1} are due to the CH stretch mode overtones. The medium intense feature at approximately 4000–4200 cm^{-1} can be assigned as the combination band ν_{OH} (ν_1) stretch plus ν_{OH} torsion (ν_{17}) and the intense feature at approximately 5378 cm^{-1} can be attributed to $\nu_1 + \text{CO}$ stretch ν_{CO} .^{38–40} The assignments are labeled in Fig. 2(b).

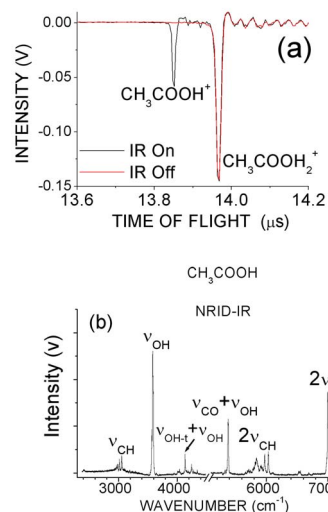


FIG. 2. (a) Mass spectrum of CH_3COOH^+ and $\text{CH}_3\text{COOH}_2^+$ with the presence of IR light (black line) and absence of IR light (red line). Note that CH_3COOH^+ intensity changes for IR on and off. (b) Mid-IR (2500–7200 cm^{-1}) vibrational spectrum of the supersonic expansion cooled acetic acid monomer detected by NRID-IR spectroscopy using acetic acid vapor seeded in 3 atm of a He/Ne mixture.

C. Nonresonant ion dip IR (NRIDip-IR) spectroscopy of the acetic acid neutral dimer (A_2)

Acetic acid is a valuable model compound for the study of cooperative hydrogen bonding as it predominantly forms well-defined cyclic dimers with two hydrogen bonds in the gas phase. This structure is presented in Fig. 3(a). The rather complicated IR and Raman spectra of the acetic acid dimer in the range of 2500–3300 cm^{-1} have been studied experimentally and theoretically since 1970.^{41–45} Mass selective NRIDip-IR spectroscopy is applied here to determine the IR spectrum of the acetic acid neutral dimer in a supersonic expansion: the spectrum of the dimer A_2 is displayed in Figs. 4(a) and 4(b). The mass channels $(\text{CH}_3\text{COOH})\text{H}^+$ and $(\text{CH}_3\text{COOH})\text{COOH}^+$ have been monitored and generate the same IR spectrum of the neutral dimer. Spectra for each mass channel are nearly identical and correspond well to each other. The IR spectrum observed monitoring $(\text{CH}_3\text{COOH})\text{H}^+$ is shown as an enhancement, while that for mass channel $(\text{CH}_3\text{COOH})\text{COOH}^+$ is shown as a decrease (dip) in the mass signal. The channel generating the $(\text{CH}_3\text{COOH})\text{COOH}^+$ species has a calculated lower ΔH of reaction than the $(\text{CH}_3\text{COOH})\text{H}^+$ channel: both channels re-

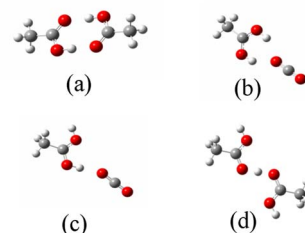


FIG. 3. Structures of the acetic acid dimer $(\text{CH}_3\text{COOH})_2$ (a), the fragment cations, m/z 105, $(\text{CH}_3\text{COOH})\text{COOH}^+$ [(b) and (c)], and $(\text{CH}_3\text{COOH})_2\text{H}^+$ (d). Geometries are optimized at the density functional theory level B3LYP/6-31G(d).

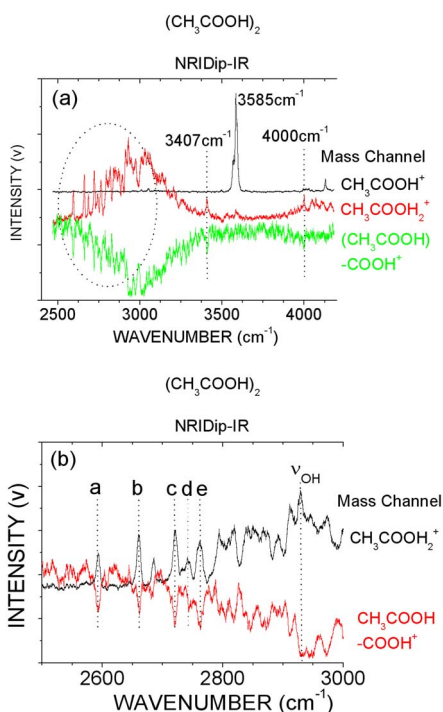
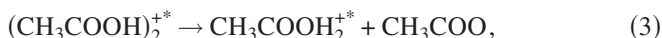


FIG. 4. Vibrational spectra of acetic acid monomer and dimer of employing NRIDip-IR spectroscopy and monitoring the mass channels CH_3COOH^+ , $\text{CH}_3\text{COOH}_2^+$, and $\text{CH}_3\text{COOHCOOH}^+$ in the region of 2500–4200 cm^{-1} (a) and 2500–3000 cm^{-1} (b). a: δ_{COH} , b: $2\delta_{\text{COH}} + \beta$, c: $2\delta_{\text{COH}} + \gamma$, d: $2\delta_{\text{COH}} + \beta$, and e: $2\delta_{\text{COH}} + \nu_{\text{OO}}$. δ_{COH} : COH bending, β : in-plane ring deformation, γ : out-of-plane ring deformation, and ν_{OO} : OO stretch.

flect the neutral dimer spectrum. The mechanism that generates a signal increase at mass channel $(\text{CH}_3\text{COOH})\text{H}^+$ and a decrease at mass channel $(\text{CH}_3\text{COOH})\text{COOH}^+$ could be as follows:



The sharp features at ~ 3407 and ~ 4000 cm^{-1} [Fig. 4(a)] could be due to the neutral dimer in an asymmetric, minor conformation with both hydrogen bonded and free OH groups. Studies have shown that the bonded OH and free CH stretches of the symmetric dimer contribute to the broad bands located approximately 3000 cm^{-1} .^{46–48} The features at 3407 and 4000 cm^{-1} can be assigned as a (weakly) bonded OH stretch and a bonded OH stretch combined with the OH torsion, respectively, for the asymmetric neutral dimer. These two features have been redshifted approximately 180 and 134 cm^{-1} from the comparable free OH stretch features of the acetic acid monomer. The broad structureless feature previously observed in the region of 2500–3000 cm^{-1} has engendered a number of different and conflicting interpretations in the past.^{16–19,49} These previous studies were carried

TABLE II. Summary assignment of the IR spectrum for the acetic acid dimer.

Modes	Energies (cm^{-1})	Assignment
$2\delta_{\text{COH}}$	2594	COH bending overtone
$2\delta_{\text{COH}} + \beta$	2661	Coupling COH bending overtone and in-plane ring deformation
$2\delta_{\text{COH}} + \gamma$	2721	Coupling COH bending overtone and out-of-planering deformation
$2\delta_{\text{COH}} + 2\beta$	2742	Coupling COH bending overtone and in-plane ring deformation overtone
$2\delta_{\text{COH}} + \nu$	2762	Coupling COH bending overtone and the OO stretches
ν_{OH}	2930	Bonded OH fundamental stretches

out on near room temperature samples and were not free of hot band interference which can add to the interpretational ambiguities. Figure 4(b) presents a better resolved spectrum in this region obtained for a supersonically cooled sample of acetic acid employing NRIDip-IR spectroscopy. The OH stretch ν_{OH} is strongly red shifted by approximately 600 cm^{-1} (peak located at 2930 cm^{-1}) due to the rather strong hydrogen bonds in the double-bridged hydrogen bonded acetic acid dimer. The peak at 2594 is assigned as the overtone of the COH bonding mode ($\delta(\text{COH})$), the IR activity of which is strongly enhanced by Fermi resonance with ν_{OH} .^{19,49} Most of the other features in this region are caused by coupling of the COH bending overtone with low frequency modes of the dimer. Features located at 2661 and 2742 cm^{-1} can be assigned as combination bands of the COH bending overtone with the in-plane ring deformation (β) and its overtone, respectively. The peaks at approximately 2721 and 2762 cm^{-1} are assigned the combination bands of the COH bending overtone with the out-of-plane ring deformations (γ) and the OO stretch mode (ν_{OO}), respectively. These assignments agree well with the recent experimental results reported by Seifert *et al.*⁴⁹ Table II summarizes these findings and assignments.

D. IR+VUV NRIDip-IR spectroscopy of acetic acid neutral clusters (A_n)

NRIDip-IR spectroscopy has been employed to obtain the vibrational spectrum of mass selected neutral clusters A_n ($n=1-8$): these spectra are monitored in the $A_{n-1}\text{H}^+$ mass channels, respectively, except for $n=1$ and 2. In these latter two instances the mass channels A^+ and ACOOH^+ are employed to acquire the monomer and dimer spectra, respectively. Figure 5 displays these data. Similar to the alcohols,²⁶ the lack of free OH features in the IR spectra for larger clusters ($n>2$) reveals that OH groups in the clusters are involved in hydrogen bonding. Only one intense dip at 3340 cm^{-1} is observed for the trimer; this represents the hydrogen bonded OH bands for the cyclic trimer. For clusters larger than the trimer, bonded OH bands have redshifted and converged to approximately 3000 cm^{-1} at $n=8$. These features then overlap with the CH bands, which apparently are not shifted upon cluster formation. The stability of the CH

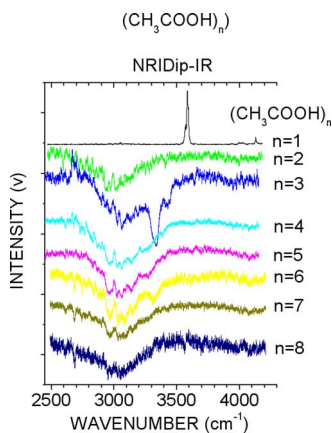


FIG. 5. The CH, OH stretch fundamental vibrations of acetic acid clusters, $(\text{CH}_3\text{COOH})_n$, for $n=1$ (top) to 8 (bottom), recorded by NRIDip-IR spectroscopy through monitoring CH_3COOH^+ ($n=1$), $(\text{CH}_3\text{COOH})\text{COOH}^+$ ($n=2$), and $(\text{CH}_3\text{COOH})_{n-1}\text{H}^+$ ($n=3-8$) signals generated by VUV single photon ionization. Here n refers to the neutral cluster whose spectrum is recorded in the above ion mass channels. The neutral cluster signals arise due to (probably multiphoton) infrared absorption and neutral cluster fragmentation.

bands suggests that the CH moieties are not directly involved in the cluster hydrogen bonding intermolecular interactions in neutral clusters.

E. IR+VUV IRPD spectroscopy of acetic acid cluster cations

Mass selected IRPD spectra of $(\text{CH}_3\text{COOH})\text{COOH}^+$ and the sequence of protonated ions $(\text{CH}_3\text{COOH})_n\text{H}^+$ ($n=1-7$) are presented in Fig. 6. Spectra are monitored in the mass channels indicated in the figure. These ions arise from the neutral $n+1$ cluster and both $(\text{CH}_3\text{COOH})\text{H}^+$ and $(\text{CH}_3\text{COOH})\text{COOH}^+$ arise from the neutral dimer. The three IR spectral features observed for the $(\text{CH}_3\text{COOH})\text{H}^+$ and $(\text{CH}_3\text{COOH})\text{COOH}^+$ mass channels (3263 , 3502 , and 3575 cm^{-1}) must arise from a common ion or two different ions with very similar spectra. Clearly the $(\text{CH}_3\text{COOH})\text{COOH}^+$ ion loses intensity and the $(\text{CH}_3\text{COOH})\text{H}^+$ ion gains intensity in the mass spectrum as the IR laser is scanned. Thus the reaction $(\text{CH}_3\text{COOH})\text{COOH}^+ \rightarrow (\text{CH}_3\text{COOH})\text{H}^+ + \text{CO}_2$ must occur

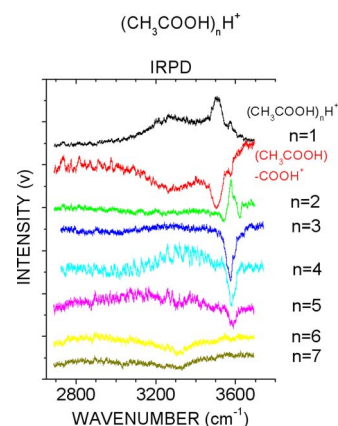


FIG. 6. The CH, OH stretch fundamental vibrations of acetic acid cluster cations, $(\text{CH}_3\text{COOH})\text{COOH}^+$, and $(\text{CH}_3\text{COOH})_n\text{H}^+$, for $n=1$ (top) to 7 (bottom), recorded by IRPD spectroscopy through monitoring the parent cation signals generated by VUV single photon ionization. Here the value n refers to the actual cluster ion observed and IR spectrum obtained, except for $(\text{CH}_3\text{COOH})\text{COOH}^+$. The ion cluster spectra arise from fragmentation of the cluster ions due to (probably multiphoton) infrared absorption (see text Sec. II for more explanation).

due to IR absorption. Figures 3(b) and 3(c) show the two isomers (I and II) for $(\text{CH}_3\text{COOH})\text{COOH}^+$ species based on B3LYP/6-31G(d) calculations. Isomer I (b) is lower in energy than isomer II (c) by 6.5 kJ/mol . The most likely explanation for the two mass channels AH^+ and ACOOH^+ displaying the same spectrum of the respective ions is that $\text{ACOOH}^+ \rightarrow \text{AH}^+$ upon absorption of IR light approximately 3000 cm^{-1} and that the spectra of AH^+ and ACOOH^+ are similar. According to the energies given in Table III for $(\text{CH}_3\text{COOH})\text{COOH}^+$, the features at 3502 cm^{-1} can be assigned as the double hydrogen bonded OH symmetric and asymmetric stretches for isomer II, and the weaker and sharp feature at 3575 and the broad band at approximately 3263 cm^{-1} can be assigned as due to the free OH stretch and the hydrogen bonded OH stretch, respectively, of isomer I.

Again, similar to the results for methanol and ethanol protonated cluster ions,²⁶ the spectrum of A_2H^+ ($n=2$ in Fig. 6) has a dip contribution from the free OH stretch at approximately 3570 cm^{-1} . This feature is distorted by a sharp peak at approximately 3575 cm^{-1} , that is generated by the dissociation of larger clusters into the protonated dimer [A_2H^+ see

TABLE III. The geometry parameters and OH vibrational energies of the isomers for the $(\text{CH}_3\text{COOH})\text{COOH}^+$ cation calculated at the theory level B3LYP/6-31G(d). Calculations are carried out with default options for GAUSSIAN 03 (energy and density minimization to 10^{-4} or energy to 10^{-5} whichever comes first for the SCF program). The integrations are accomplished with a “fine” grid as default. All energies are corrected for harmonic zero point energies.

Parameter		Isomer I	Isomer II
Hydrogen bond	Bond length ($R_{\text{O-H}\cdots\text{O}}$) (Å)	2.71	2.82
	Bond angle ($\angle\text{O-H}\cdots\text{O}$) (°)	177.8	149.8
Stretch energies	Bonded OH (cm^{-1})	3337	(3263) ^a , 3549, 3492 ^b (3502) ^a
	Free OH (cm^{-1})	3608	3575 ^a
Energy different (kJ/mol)		6.5	

^aThe values in the parentheses are the experimental values obtained in this work.

^bSymmetric and asymmetric stretches.

Fig. 3(d)] mass channel. This observation implies that the protonated dimer has a stable closed shell structure: as can be seen in Fig. 3(d) this species has a structure in which the proton is shared symmetrically between the two acetic acid molecules in the cluster. For medium size protonated clusters ($n=3, 4$, and 5), a relatively sharp feature at approximately 3575 cm^{-1} ($n=3$), 3579 cm^{-1} ($n=4$), and 3586 cm^{-1} ($n=5$) is observed and assigned as the free OH stretch in these protonated clusters. This free OH band, however, for $A_n\text{H}^+$ ($n=3, 4$, and 5) disappears at $n=6$ and a weak broad band approximately 3320 cm^{-1} can be observed for this latter protonated cluster ion. These results suggest the formation of closed cyclic or multicyclic structure(s) for protonated acetic acid clusters with $n \geq 6$. Similar results are found for methanol clusters.⁵⁰

IV. CONCLUSIONS

The TOFMS of acetic acid hydrogen bonded clusters in a supersonic expansion is recorded with 118 nm VUV ionization of neutral clusters. The primary sequence of clusters observed in the mass spectrum is $(\text{CH}_3\text{COOH})_n\text{H}^+$. Additionally, one cluster of the form $(\text{CH}_3\text{COOH})\text{COOH}^+$ is observed. The latter cluster arises from the neutral dimer by the loss of CH_3 upon ionization. The main sequence of clusters arises from the $(\text{CH}_3\text{COOH})_{n+1}$ neutral through proton transfer and fragmentation following ionization to $(\text{CH}_3\text{COOH})_{n+1}^+$. The absence of other fragment ions of the form $(\text{CH}_3\text{COOH})_n\text{COOH}^+$ from larger neutrals $(\text{CH}_3\text{COOH})_{n+1}$ ($n > 2$) suggests that the proton affinities of larger clusters are larger than that of the neutral monomer.

The fundamental and first overtone of the CH and OH stretch modes and some combination bands are identified in the spectrum of cooled acetic acid between 2500 and 7500 cm^{-1} , through IR+VUV nonresonance ionization spectroscopy.

Mass resolved IR spectra of acetic neutral clusters are obtained in the range of $2500\text{--}3800\text{ cm}^{-1}$ employing nonresonant ion dip IR spectroscopy. Characteristic bands observed at approximately 2500 to 2900 cm^{-1} for the cyclic dimer are identified. IR spectra for larger clusters suggest that all $(\text{CH}_3\text{COOH})_n$ neutral clusters form a cyclic structure, with all OH groups involved in the cluster hydrogen bonding network. The CH groups are not involved in the hydrogen bonding cluster network.

Spectra obtained for the protonated acetic acid clusters ($n=1\text{--}7$) show that the free OH stretches exhibit a blueshift with increasing cluster size n and converge to a value of approximately 3580 cm^{-1} for $n=5$. Thus at least one OH group in each member of the protonated cluster ion series $A_n\text{H}^+$ ($1 \leq n \leq 5$) is not involved in the cluster hydrogen bonding network. The disappearance of the free OH band at approximately 3580 cm^{-1} and the appearance of a broad and weak band at approximately 3350 cm^{-1} for $n \geq 6$ suggests that closed cyclic or multicyclic structures are formed for protonated acetic acid cluster ions $(\text{CH}_3\text{COOH})_n\text{H}^+$ ($n \geq 6$).

ACKNOWLEDGMENTS

Research described in this article was supported in part by Philip Morris USA, Inc. and by Philip Morris International. These studies have also been supported by the US-NSF.

- ¹L. Leiserowitz, Acta Crystallogr., Sect. B: Struct. Crystallogr. Cryst. Chem. **B32**, 775 (1976).
- ²K. D. Cook and J. W. Taylor, Int. J. Mass Spectrom. Ion Phys. **35**, 259 (1980).
- ³Y. Mori and T. Kitagawa, Int. J. Mass Spectrom. Ion Process. **64**, 169 (1985).
- ⁴Y. Mori and T. Kitagawa, Int. J. Mass Spectrom. Ion Process. **84**, 305 (1988).
- ⁵Y. Mori and T. Kitagawa, Int. J. Mass Spectrom. Ion Process. **84**, 319 (1988).
- ⁶R. Sievert, I. Cadez, J. Van Doren, and A. W. Castleman, Jr., J. Phys. Chem. **88**, 4502 (1984).
- ⁷R. G. Keesee, R. Sievert, and A. W. Castleman, Jr., Ber. Bunsenges. Phys. Chem. **88**, 273 (1984).
- ⁸M. Meot-Ner, J. Am. Chem. Soc. **114**, 3312 (1992).
- ⁹M. Tsuchiya, S. Teshima, A. Shigihara, and T. J. Hirano, J. Mass Spectrom. Soc. Jpn. **46**, 483 (1998).
- ¹⁰N. Nishi, T. Nakabayashi, and K. Kosugi, J. Phys. Chem. A **103**, 10851 (1999).
- ¹¹J. Karle and L. O. Brockway, J. Am. Chem. Soc. **66**, 574 (1944).
- ¹²T. Nakabayashi, K. Kosugi, and N. Nishi, J. Phys. Chem. A **103**, 8595 (1999).
- ¹³W. Y. Feng and C. Lifshitz, J. Phys. Chem. **98**, 6075 (1994).
- ¹⁴C. Lifshitz and W. Y. Feng, Int. J. Mass Spectrom. Ion Process. **146/147**, 223 (1995).
- ¹⁵R. Zhang and C. Lifshitz, J. Phys. Chem. **100**, 960 (1996).
- ¹⁶R. L. Redington and C. L. Kenneth, J. Chem. Phys. **54**, 4111 (1971).
- ¹⁷Y. Grenie, J.-C. Cornut, and J.-C. Lassegues, J. Chem. Phys. **55**, 5844 (1971).
- ¹⁸C. Emmeluth, M. A. Suhm, and D. Luckhaus, J. Chem. Phys. **118**, 2242 (2003).
- ¹⁹J. Dreyer, J. Chem. Phys. **122**, 184306 (2005).
- ²⁰V. Aviyente, R. Zhang, T. Varnali, and C. Lifshitz, Int. J. Mass Spectrom. Ion Process. **161**, 123 (1997).
- ²¹L. I. Yeh, M. Okumura, J. D. Myers, J. M. Price, and Y. T. Lee, J. Chem. Phys. **91**, 7319 (1989).
- ²²E. J. Bieske and J. P. Maier, Chem. Rev. (Washington, D.C.) **93**, 2603 (1993).
- ²³J. M. Lisy, *Cluster Ions* (Wiley, Chichester, 1993), p. 217.
- ²⁴K. Ohashi, H. Izutsu, Y. Inokuchi, K. Hino, N. Nishi, and H. Sekiya, Chem. Phys. Lett. **321**, 406 (2000).
- ²⁵K. Ohashi, Y. Inokuchi, H. Izutsu, K. Hino, N. Yamamoto, and H. Sekiya, Chem. Phys. Lett. **323**, 43 (2000).
- ²⁶Y. J. Hu, H. B. Fu, and E. R. Bernstein, J. Chem. Phys. **125**, 154306 (2006).
- ²⁷H. B. Fu, Y. J. Hu, and E. R. Bernstein, J. Chem. Phys. **124**, 024302 (2006).
- ²⁸(a) Q. Y. Shang, P. O. Moreno, and E. R. Bernstein, J. Am. Chem. Soc. **116**, 311 (1994); (b) Q. Y. Shang and E. R. Bernstein, J. Chem. Phys. **100**, 8625 (1994); (c) R. Disselkamp, E. R. Bernstein, J. I. Seeman, and H. V. Secor, *ibid.* **97**, 8130 (1992); (d) F. Dong, S. Heinbuch, J. J. Rocca, and E. R. Bernstein, *ibid.* **124**, 224319 (2006).
- ²⁹Y. J. Hu, H. B. Fu, and E. R. Bernstein, J. Phys. Chem. A **110**, 2629 (2006).
- ³⁰<http://webbook.nist.gov/chemistry>
- ³¹B. H. Torrie, S. X. Weng, and B. M. Powell, Mol. Phys. **67**, 575 (1989).
- ³²T. Yamaguchi, K. Hidaka, and A. K. Soper, Mol. Phys. **97**, 603 (1999).
- ³³S. Sarkar and R. N. Joarder, J. Chem. Phys. **99**, 2032 (1993).
- ³⁴A. Arencibia, M. Taravillo, F. J. Perez, J. Nunez, and V. G. Baonza, Phys. Rev. Lett. **89**, 195504 (2002).
- ³⁵S.-T. Tsai, J.-C. Jiang, M.-F. Lin, Y. T. Lee, and C.-K. Ni, J. Chem. Phys. **120**, 8979 (2004).
- ³⁶K. R. Lange, N. P. Wells, K. S. Plegge, and J. A. Phillips, J. Phys. Chem. A **105**, 3481 (2001).
- ³⁷C. Emmeluth and M. A. Suhm, Phys. Chem. Chem. Phys. **5**, 3094 (2003).

- ³⁸D. K. Havey, K. J. Feierabend, J. C. Black, and V. Vaida, *J. Mol. Spectrosc.* **229**, 151 (2005).
- ³⁹E. M. S. Maçôas, L. Khriachtchev, R. Fausto, and M. Räsänen, *J. Phys. Chem.* **108**, 3380 (2004).
- ⁴⁰E. M. S. Maçôas, L. Khriachtchev, M. Pettersson, R. Fausto, and M. Räsänen, *J. Am. Chem. Soc.* **125**, 16188 (2003).
- ⁴¹R. L. Redington and K. C. Lin, *J. Chem. Phys.* **54**, 4111 (1971).
- ⁴²Y. Marechal, *J. Chem. Phys.* **87**, 6344 (1987).
- ⁴³K. Fukushima and B. Zwolinski, *J. Chem. Phys.* **50**, 737 (1969).
- ⁴⁴L. Turi and J. J. Dannenberg, *J. Phys. Chem.* **97**, 12197 (1993).
- ⁴⁵L. Turi, *J. Phys. Chem.* **100**, 11285 (1996).
- ⁴⁶C. Emmeluth, M. A. Suhm, and D. Luckhaus, *J. Chem. Phys.* **118**, 2242 (2003).
- ⁴⁷C. A. Southern, D. H. Levy, J. A. Stearns, G. M. Florio, A. Longarte, and T. S. Zwier, *J. Phys. Chem. A* **108**, 4599 (2004).
- ⁴⁸J. Chocholousova, J. Vacek, and P. Hobza, *J. Phys. Chem. A* **107**, 3086 (2003).
- ⁴⁹G. Seifert, T. Patzlaff, and H. Graener, *Chem. Phys. Lett.* **333**, 248 (2001).
- ⁵⁰A. Fujii, S. Enomoto, M. Miyazaki, and N. Mikami, *J. Phys. Chem. A* **109**, 138 (2005).